World Journal of Engineering and Technology, 2023, 11, 663-671
https://www.scirp.org/journal/wjet
ISSN Online: 2331-4249
ISSN Print: 2331-4222

Assessment of Modeling Collimator Designs for Gamma-Ray Transmission of Uranium Oxide Spectrometry Using HPGe Detectors

Rasha Ali El-Tayebany, Hekmat Elbegawy

Nuclear and Radiological Safety Research Center, Egyptian Atomic Energy Authority, Cairo, Egypt
Email: rreltyebany@gmail.com

How to cite this paper: El-Tayebany, R.A. and Elbegawy, H. (2023) Assessment of Modeling Collimator Designs for Gamma-Ray Transmission of Uranium Oxide Spectrometry Using HPGe Detectors. *World Journal of Engineering and Technology*, **11**, 663-671.
https://doi.org/10.4236/wjet.2023.114044

Received: August 7, 2023
Accepted: September 19, 2023
Published: September 22, 2023

Abstract

Many scientific domains use gamma-ray spectrometry, but non-destructive gamma scanning and gamma emission tomography of radioactive fuel in particular. In the experimental setting, a collimator is frequently employed to focus on a particular location of interest in the fuel. Predictive models for the transmitted gamma-ray intensity through the collimator are required for both the optimization of instrument design and the planning of measurement campaigns. Gamma-ray transport accuracy is frequently predicted using Monte Carlo radiation transport methods, but using these tools in low-efficiency experimental setups is challenging due to the lengthy computation times needed. This study focused on the full-energy peak intensity that was transmitted through several collimator designs, including rectangle and cylinder. The rate of photons arriving at a detector on the other side of the collimator was calculated for anisotropic source of SNM (U_3O_8). Some geometrical assumptions that depended on the source-to-collimator distance and collimator dimensions (length, radius or length, height, and width) were applied to achieve precise findings.

Keywords

Monte Carlo, High Purity Germanium (HPGe), Collimator, Uranium

1. Introduction

In several scientific disciplines, gamma-ray spectroscopy is a commonly utilized technique. It is utilized in a variety of fields, including nuclear technology and fundamental physics research. The application of gamma-ray spectroscopy in non-destructive nuclear fuel inspections is used e.g. gamma scanning and Gamma Emission Tomography [1]. In particular, the latter is increasingly considered for use in nuclear fuel tests as well as in nuclear safeguards [2]-[7]. In these situations, the measuring devices consist of a high energy resolution detector and a collimator, where the collimator enables the investigation of well-defined fuel zones. The geometry and material composition of the collimator should be carefully considered during the beginning stages of creating a spectroscopic system since they have a significant impact on the system's performance. MC simulations are frequently used to produce outcomes with the potential for high accuracy [8] [9] [10]. For instance, for an isotopically emitting point source positioned directly in front of the collimator opening, the likelihood of a gamma ray reaching the opposite opening is on the order of 10^{-9} for a collimator with a square slit that is 80 cm long and 0.1 cm wide. The probability of penetration can be substantially smaller for the parts of a fuel object that are not directly in front of the opening or further away. As a result, MC approaches need a lot of photons to be sampled, which can be time-consuming if no special variance reduction techniques are used, such as those proposed by. The Monte Carlo radiation transport code MCNP6 is used to model a mono-directional source, and correction factors are added to account for the effects of a cylindrical aperture and solid-angle effects of isotropic emission [10] [11].

The nondestructive assay (NDA) of radioactive waste detection uses a technique called Tomographic Gamma Scanning (TGS), which is relatively recent [1] [2] [3] [4] [5]. It helps to resolve the issue of invalid attenuation correction brought on by the unequal distribution of the sample medium in industrial CT imaging technologies. As a result, it increases the precision of the information contained in the non-uniform analysis of radioactive materials in the measurements of gamma ray spectroscopy [6] [7] [8] [9]. With a high sample throughput and sensitivity, the TGS approach seeks to produce precise measurements of radionuclides with low specific activity. The image quality, in the sense it is generally understood, is of little concern beyond its effect on assay accuracy. In some research outcomes, a TGS design study was conducted to enhance the functionality and other tomographic assay systems. The study was based on computer simulations. The investigation of the distribution of the various gamma-ray emitting isotopes typically present in irradiated nuclear fuel is made possible by the use of a high-resolution HPGe detector in the measurements, which enables the collection of detailed gamma-ray spectra from which any peak present may be chosen for tomographic reconstruction. The number of counts gathered in a specific gamma-ray peak is significantly more than the number of counts contained in the peak in a single spectrum because gamma spectra are recorded at between 8000 and 25,000 points surrounding the fuel. As a result, usable images can be created from even peaks in a single spectrum that has a relatively small number of counts [12] [13].

In this article, we describe the findings of a collimator design study that was conducted to enhance the functionality of safeguards measurements and tomographic assay systems. The study was based on Monte Carlo simulations to calculate the HPGe detector efficiency. Usually, the absolute efficiency is determined by the pulse-height tally (F8) of each photon emitted from the source. The focus of this work is on the associated problems with collimator design.

2. Theoretical Model

The count rate, CR, in the detector of a spectroscopic system can be described as a function of the source activity A, the emission intensity, and the gamma-ray energy per decay of the gamma line I_γ, the geometric efficiency ε_g, and the detector intrinsic full-energy peak efficiency, ε_d, as expressed in Equation (1)

$$CR = AI_\gamma \varepsilon_g \varepsilon_d \quad (1)$$

By using this expression, the amount of counts in the gamma-ray spectrum's full-energy peak can be used to experimentally evaluate a sample's activity. Notably, depending on the measurement settings, a number of correction factors, such as self-attenuation in the object, count rate-related effects, or real coincidence summing, may be necessary for accurate results. The geometric efficiency ε_g, meaning the probability per photon to reach the detector, is in this case determined by the collimator slit dimensions and the collimator-source distance.

Typically, just a small portion of the source plane is covered by the collimator slit. Because of this, it is more useful to express the count rate intensity based on the source's planar activity concentration, adapted from [14], as shown in Equation (2) below:

$$CR = \int x_S \int y_S A_{sur} I_\gamma \varepsilon_g \left(E_\gamma, x_S, y_S\right) \varepsilon_d \mathrm{d}x_S \mathrm{d}y_S, \quad (2)$$

We have different geometrical designs for testing which are the (cylinder & rectangle) shapes with different dimensions that are carried out. The cylindrical shapes are designed with different diameters and heights while the rectangular shape is designed with different lengths, widths, and heights. We assumed six designs as shown in **Table 1**. The first three designs with design ID: Dx, Dy, and Dz refer to cylindrical shapes with different diameters and heights while, the other three designs that are with design ID: Dx', Dy', and Dz' refer to the rectangular shape with different dimensions in height, length, and width. Each design in the cylindrical shape with a fixed diameter is simulated with different four heights (H1, H2, H3, and H4).

3. Simulation Setups

The MCNP code can only analyze an issue in the form that it is given; it cannot tell when the wrong material has been specified or when the geometry has been inaccurately modeled. Keep in mind that without knowledge of the problem's context, the standard of the solution, and a reasonable expectation of the outcome and its associated confidence interval with MCNP or any other code is useless [15] [16] [17].

In this section, the simulated design for the collimator is described with detailed dimensions and configuration. **Figure 1** describes the simulated setup where the standard nuclear material (SNM), collimator, and HPGe detector are

Table 1. Detailed dimensions of collimator designs.

	Cylindrical shape			Rectangular shape	
Design ID	Diameter (cm)	Height (cm) H1, H2, H3, H4	Design ID	L × W (cm)	Height (cm) H1, H2, H3, H4
Dx	1	5, 10, 15, 20	Dx'	1 × 1	5, 10, 15, 20
Dy	2	5, 10, 15, 20	Dy'	1.5 × 1.5	5, 10, 15, 20
Dz	3	5, 10, 15, 20	Dz'	2 × 1.5	5, 10, 15, 20

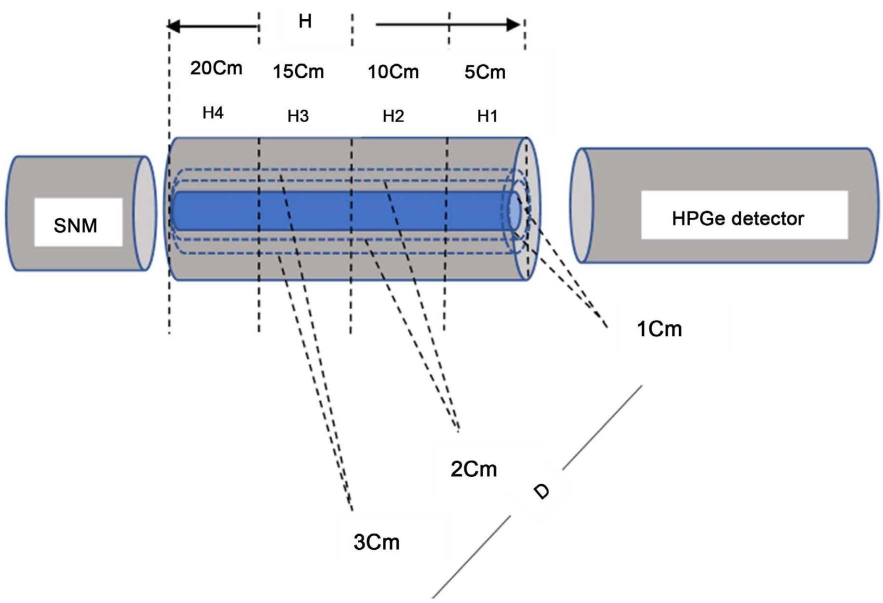

Figure 1. Collimator design (cylindrical shape).

on the same alignment and the distance between each one is 3 cm. The measuring system is composed of: A high purity planar HPGe detector (Canberra; model GL0515R), active area = 500 mm^2) 540 eV FWHM resolution at 2 keV, a Spectroscopy Pre-amplifier [model 2002 CPSL], a Cryostat (model 7905 SL-5) liquid nitrogen Dewar, an adjustable High-Voltage Power Supply (HV-PS) Inspector Multi-Channel Pulse-height Analyzer (MCA) module (model 1200 IMCA) and built-in amplifier, a 100-MHZ Wilkinson ramp Amplitude-to-digital Converter (ADC), and an online microcomputer data acquisition module for the control and analysis [18] [19]. The SNM compose of a compact powder of Uranium oxide (U_3O_8) with a total weight of 200.1 gm and covered with Al- can [20]. The experimental work is applied by using the SNM sample with an enrichment 4.46% and the observed energy line is at 185.7 keV. The whole shape of the can is simulated in the input file of the MCNP code. Figure 1, Figure 2 presents the whole configuration of the simulated set up including the different shapes of collimators (cylindrical and rectangle) with different dimensions in diameter (D) and length (L), for cylindrical shape while the rectangular shape with different length, width (W) and height (H).

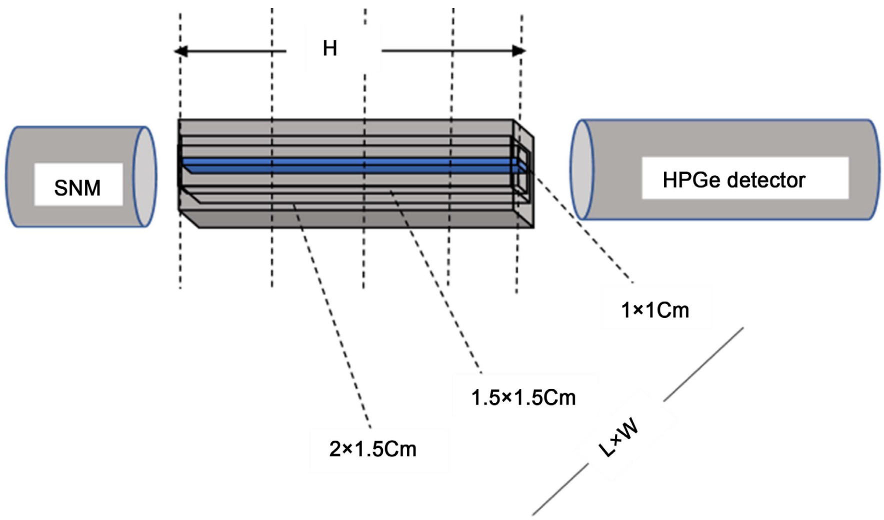

Figure 2. Collimator design (rectangular shape).

Where, the above parameters are required for the simulation and the detailed data are illustrated in Table 2. The collimator designs that take design ID: Dx1, Dx2 and Dx3 have the same diameter which is equal to 1 cm with various height (H) that are taking the values from 5 to 20 cm. Similarly, the designs with design ID: Dy1, Dy2 and Dy3 that have the same diameter 2 cm with different heights and finally, the collimator designs Dz1, Dz2 and Dz3 have the same diameter 3 cm. on the other side, the designs that take rectangular shapes such as; Dx1', Dx2' and Dx3' have the same length (L) = 1 cm and width (W)= 1 cm with different H from 5 to 20 cm. Also, Dy1, Dy2, and Dy3 have L × W = 1.5 × 1.5 with a height from 5 - 20 cm.

4. Results

The simulation of the configuration shows that varying dimensions for collimator designs. The magnitude of the gamma current that reaches the detector exceeds several orders of magnitude. A good overall agreement was noted with the MCNP6simulations, including a perfectly performing collimator, and taking into account significant parameters such as; solid angle, attenuation, and geometrical efficiency that depends on the distance between the source and collimator and the dimensions of the collimator itself. Note that the simulations have been run with the same starting seed, to better observe the trend of the intensity variations due to the geometry of the setup. The input files are created for each collimator design to estimate pulse height distribution (F8). Figure 3 shows the effect of each design on the pulse height distribution where Dz denotes to change of height values for the cylindrical design with a fixed diameter 1 cm and Dy describes the change of height values for the cylindrical design with a fixed diameter 2 cm and Dz describes the change of height values for the cylindrical design with a fixed diameter 3 cm. Also, the identical idea is performed for the rectangular design Dx', Dy', Dz'.

Table 2. The required parameters that needed in MCNP6 input files.

	Design ID (Cylindrical shape)	Dimensions (H, D)	Design ID (Rectangular shape)	Dimensions (H, L × W)
Sample ID SRM969-446	Dx1	5, 1	Dx1'	5, 1 × 1
	Dx2	10, 1	Dx2'	10, 1 × 1
	Dx3	15, 1	Dx3'	15, 1 × 1
	Dx4	20, 1	Dx4'	20, 1 × 1
	Dy1	5 , 2	Dy1'	5, 1.5 × 1.5
	Dy2	10, 2	Dy2'	10, 1.5 × 1.5
	Dy3	15, 2	Dy3'	15, 1.5 × 1.5
	Dy4	20, 2	Dy4'	20, 1.5 × 1.5
	Dz1	5, 3	Dx1'	5, 2 × 1.5
	Dz2	10, 3	Dx1'	10, 2 × 1.5
	Dz3	15, 3	Dx1'	15, 2 × 1.5
	Dz4	20, 3	Dx1'	20, 2 × 1.5

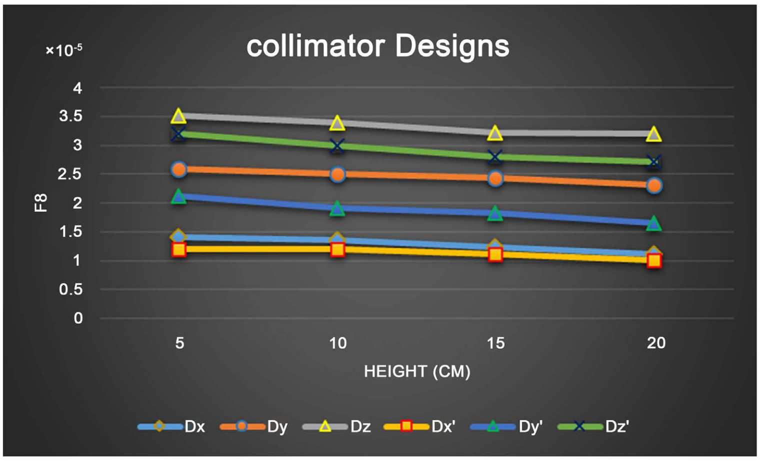

Figure 3. Correlation between collimator height with F8 tally.

The results of the MCNP6 validation simulations including the penetrating gamma component crossing the collimator bulk material, show that different values for F8, are systematically underestimating the pulse height distribution observed by the detector. This might have been expected since the variance reduction techniques have been used to overcome the ling estimation time in the input file and give us more precise results that should be obtained. In Figure 4, the Difference between the experimental and simulated results in both shapes is presented. We found here that largest differences are in rectangular collimator shapes that is because of the corners of the collimator which cause multiple scattering that leads to decreasing in interested photon energy.

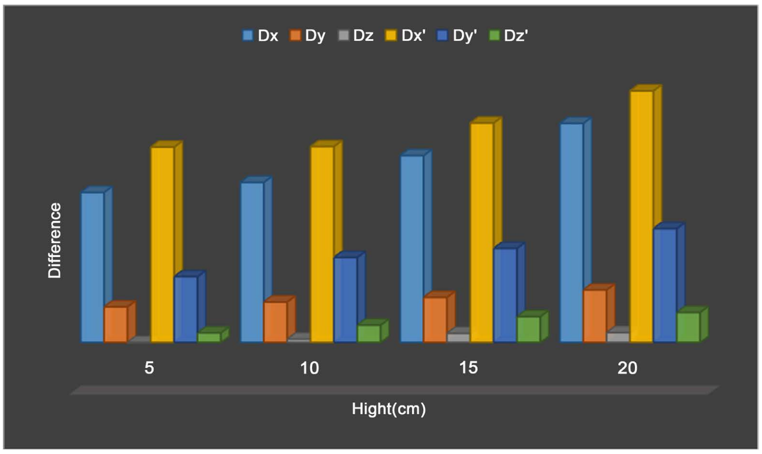

Figure 4. Difference results between the experimental and simulation.

5. Conclusion

Monte Carlo simulations have been carried out to design a collimator to improve the performance of the measurement system. The simulation results reveal that the cylindrical shape design for the collimator with ID: Dy has a diameter of 2 cm and a height range from 5 to 20 cm and it gives the acceptable difference in the range of 3.5% - 5% in the optimal shape. The optimal shape of the detector collimator was determined with the same collimator aperture radius and height. The rectangular shape of the collimator is considered the worst that's because of the corners of the collimator which cause multiple scattering that leads to a decrease in interested photon energy. Since an HPGe detector was used in the measurements the collected gamma-ray spectra had high resolution and contained many peaks which are therefore available for tomographic reconstruction and analysis. The improvement of spatial resolution for the spectrum utilising the chosen collimator designs is the suggested direction for future research.

Conflicts of Interest

The authors declare that they have no known competing financial interests or personal relationships that could have appeared to influence the work reported in this paper.

References

[1] Willman, C., Håkansson, A., Osifo, O., Bäcklin, A. and Jacobsson Svärd, S. (2005) Nondestructive Assay of Spent Nuclear Fuel with Gamma-Ray Spectroscopy. *Annals of Nuclear Energy*, **33**, 427-438. https://doi.org/10.1016/j.anucene.2005.12.005

[2] Virta, R., Backholm, R., Bubba, T.A., Helin, T., Moring, M., Siltanen, S., Dendooven, P. and Honkamaa, T. (2020) Fuel Rod Classification from Passive Gamma Emission Tomography (PGET) of Spent Nuclear Fuel Assemblies. https://arxiv.org/abs/2009.11617

[3] Jansson, P., Jacobsson, Svärd, S., Håkansson, A. and Bäcklin, A. (2006) A Device for Nondestructive Experimental Determination of the Power Distribution in a Nuclear Fuel Assembly. *Nuclear Science and Engineering*, **152**, 76-86.

https://doi.org/10.13182/NSE06-A2565

[4] Caruso, S. (2007) Characterisation of High-Burnup LWR Fuel Rods through Gamma Tomography. École Polytechnique Fédérale de Lausanne, Lausanne, Switzerland. https://infoscience.epfl.ch/record/100031

[5] Holcombe, S., Jacobsson Svärd, S. and Hallstadius, L. (2015) A Novel Gamma Emission Tomography Equipment for Enhanced Fuel Characterization Capabilities within the OECD Halden Reactor Project. *Annals of Nuclear Energy*, **85**, 837-845. https://doi.org/10.1016/j.anucene.2015.06.043

[6] Schulthess, J., Woolstenhulme, N., Craft, A., Kane, J., Boulton, N., Chuirazzi, W., Winston, A., Smolinski, A., Jensen, C., Kamerman, D. and Wachs, D. (2020) Non-Destructive Post-Irradiation Examination Results of the First Modern Fueled Experiments in TREAT. *Journal of Nuclear Materials*, **541**, 152442. https://doi.org/10.1016/j.jnucmat.2020.152442

[7] Shiba, S. and Sagara, H. (2021) Passive Gamma Emission Tomography with Ordered Subset Expectation Maximization Method. *Annals of Nuclear Energy*, **150**, Article 107823. https://doi.org/10.1016/j.anucene.2020.107823

[8] Smith, E.L., Jacobsson, S., Mozin, V. and Jansson, P. (2016) A Viability Study of Gamma Emission Tomography for Spent Fuel Verification: JNT 1955 Phase I. Technical Report, PNNL-25995. http://urn.kb.se/resolve?urn=urn:nbn:se:uu:diva-306584

[9] Kähkönen, T. (2021) Evaluating the Viability of Serpent in Passive Gamma Emission Tomography (PGET) Radiation Transport Simulations. Special Assignment Report, Aalto University, Finland. https://aaltodoc.aalto.fi:443/handle/123456789/102716

[10] Kilby, S., Jin, Z., Avachat, A., *et al.* (2019) A Source Biasing and Variance Reduction Technique for Monte Carlo Radiation Transport Modeling of Emission Tomography Problems. *Journal of Radioanalytical and Nuclear Chemistry*, **320**, 37-45. https://doi.org/10.1007/s10967-019-06457-1

[11] Andersson, P., Holcombe, S. and Tverberg, T. (2016) Inspection of a LOCA Test Rod at the Halden Reactor Project Using Gamma Emission Tomography. *Top Fuel—LWR Fuels with Enhanced Safety and Performance*, Boise, 11-16 September 2016. http://urn.kb.se/resolve?urn=urn:nbn:se:uu:diva-303810

[12] Holcombe, S. and Andersson, P. (2016) Gamma Emission Tomography Measurements of Fuel Assemblies at the Halden Reactor. *Top Fuel—LWR Fuels with Enhanced Safety and Performance*, Boise, 11-15 September 2016, 1601-1611. http://urn.kb.se/resolve?urn=urn:nbn:se:uu:diva-303812

[13] Gilmore, G.R. (2008) Practical Gamma-Ray Spectroscopy. John Wiley & Sons, Inc., Hoboken. https://doi.org/10.1002/9780470861981

[14] Jacobsson Svärd, S. (2004) A Tomographic Measurement Technique for Irradiated Nuclear Fuel Assemblies. Acta Universitatis Upsaliensis, Uppsala. http://urn.kb.se/resolve?urn=urn:nbn:se:uu:diva-4227

[15] Werner, C.J. (2017) MCNP Users Manual—Code Version 6.2. Report la-UR-17-29981, Los Alamos National Laboratory.

[16] Shultis, J.K. and Faw, R.E. (2011) An MCNP Primer. Kansas State University, Manhattan, KS.

[17] Leppänen, J., *et al.* (2015) The Serpent Monte Carlo Code: Status, Development and Applications in 2013. *Annals of Nuclear Energy*, **82**, 142-150. https://doi.org/10.1016/j.anucene.2014.08.024

[18] Canberra Industries (1995) Germanium Detectors, User's Manual, USA.

[19] Canberra (1996) Detector Specification and Performance Data (HPGe Model GL0515R-7905SL-5) USA.

[20] USA-National Bureau of Standards, Standard Reference Material 969 (2006) Uranium Isotopic Reference Material for Gamma Spectrometry Measurements. USA-Eckert & Ziegler, California, USA.